1 Introduction

Light-matter interaction is a fundamental process underlying many physical phenomena and a diverse range of technological applications. This interaction, driven by the exchange of energy between electromagnetic fields and matter excitations, has become a focal point across disciplines such as materials science, energy research, and is especially important in optics and photonic quantum technologies [1–4]. For future telecommunications applications, it is critical to move from bulky laboratory setups to miniaturized on-chip photonic devices that are essential for practical use of quantum systems [5]. For example, plasmonic antennas can be designed to couple to specific radiative modes [6], enabling highly directional emission from quantum emitters [7, 8].

The interaction between such a quantum emitter, i.e. a two-level system and a confined electromagnetic field can be classified into weak and strong coupling regimes, depending on the strength of the coupling or g-factor [9–11]. Light-matter interaction can be enhanced by two fundamentally different approaches, each with its own unique advantages and limitations. First, the interaction time can be increased by minimizing losses in resonators, leading to extremely large quality factors Q [12]. On the other hand, the interaction probability can be increased by reducing the mode volume V, e.g. through resonant polariton-based near-field interactions in open cavities or antenna systems [13, 14]. Among the most effective methods to achieve small mode volumes are surface plasmon polaritons in metals, which arise from the collective oscillations of free electrons coupled to visible light [15]. In particular, resonant plasmonic antennas combine extremely high radiative decay rates of quantum emitters due to their small mode volumes with broadband operation, due to their moderate Q factors [14].

The increasing ability to fabricate structures with nanometer precision significantly advances the field of plasmonics and photonics in this regard. Focused particle beam techniques using electrons or ions are becoming fundamental to nanotechnology and materials science, providing unprecedented spatial control over mask processing, as well as direct material deposition and removal [16, 17].

Focused electron beam induced deposition, also known as direct electron beam writing, provides nanometer resolution by leveraging the fine control of electron microscopes. The technique has evolved significantly since it was first demonstrated in 1976 by writing

thin carbon wires based on the localized decomposition of residual hydrocarbons in a vacuum chamber [18]. Today, direct electron beam writing is utilized in various highly specialized applications such as magnetic force microscopy [19], nanomagnetics [20], superconducting circuits [21], optical metamaterials [22], plasmonics [23, 24], and diverse sensing applications [25–30].

While focused ion beams can be used in the same way for deposition, among various other techniques [17], we are particularly interested in localized material sputtering for patterning planar structures. A typical application is to remove material on a small scale, that cannot be easily removed by other techniques, such as milling of well-defined holes in fully processed chip devices, for example, in EPR-on-chip detectors [31]. In optics, focused ion beam processing is instrumental in the prototyping of photonic crystals [32] and in the precise shaping of metallic plasmonic structures [33]. Similarly, FIB can be used to fabricate phononic crystals in suspended 2D materials such as graphene or MoS_2 [34], or to mill a solid immersion lens around single-photon emitter in diamond to enhance the light outcoupling [35]. Ion beams can even be used to create defects in crystals that function as single-photon sources [36].

This work focuses on nanoscale helical plasmonic devices fabricated by direct 3D writing using both charged particle beams, namely a double plasmonic helix and a polarization converter device. Such structures offer control over the polarization state of light, an important parameter in modern telecommunications and quantum optics [5]. The double helix serves as a highly directional antenna for circularly polarized light, while in the polarization converter, the double helix is coupled to a plasmonic waveguide that allows circular to linear polarization conversion.

Sometimes fundamental research unveils unexpected new insights in interrelated fields. The thesis concludes with a chapter discussing electron beam-based seeding, which enables area-selective autocatalytic growth of gold films. As shown in earlier works, an electron beam can be used to enable area selectivity of thin film deposition of certain metals [37, 38]. However, a true area-selective deposition of gold without the need for preliminary lithography remained elusive for a long time. Here, the autocatalytic property of the precursor $Au(acac)Me_2$ is exploited for the first time to realize area-selective deposition of thin gold films on arbitrary geometries in a relatively low-temperature process.

The thesis is organized as follows:

- Chapter 2 introduces the reader to the basic concepts of electromagnetism and plasmonics. The chapter also describes full-field electrodynamic modeling and its usefulness for studying plasmonic devices.

- Chapter 3 provides an introduction to the fabrication and characterization techniques used in this thesis.
- Chapter 4 is dedicated to the double helical antenna. Double helices are introduced, analyzed with full-field simulations, fabricated by direct electron beam writing, and finally optically characterized in transmission optical setup.
- Chapter 5 presents a linear-to-circular polarization plasmonic converter based on a two-wire transmission line and the double helix. A coupling between two components is optimized by full-field modeling, and the final device is fabricated by both focused ion and electron beams.
- In chapter 6, area-selective chemical vapor deposition of gold by seeding with electron beam is presented. This technique allows selective gold deposition at relatively low temperatures and can be exploited to estimate the temperature, induced by the electron beam.
- Chapter 7 summarizes key findings and contributions of the work, while also providing an outlook for future studies and potential applications.

2 Theoretical background

One of the main objectives of this thesis is to design a device capable of converting a linear polarization state of light into a circular polarization state with very small dimensions. To provide a basis for understanding the optics of metal nanostructures, this chapter introduces key concepts derived from Maxwell's equations with a focus on plasmonics - the interaction between electromagnetic fields and free electron gas in metals. Plasmonics enables significant miniaturization through extreme light confinement and has applications in enhancing sensor sensitivity, improving the efficiency of photovoltaic devices, and miniaturizing photonic circuits, making it a focal area of research in nanotechnology and materials science. This chapter also provides a brief overview of two numerical methods for solving Maxwell's equations that will be used to design and optimize plasmonic antennas and waveguides.

2.1 Key concepts of electromagnetism

Plasmonics and optical scattering are subsets of electromagnetic theory based on Maxwell's equations. The beauty of plasmonics lies in its almost complete description by classical physics. The interested reader will find more detailed information in specialized books on electromagnetic problem [15, 39, 40]. This section presents the necessary mathematical and physical tools in a simplified and consolidated manner.

2.1.1 Maxwell's and wave equations

Just as any grand journey begins with a single step, our introduction to electromagnetism begins with Maxwell's equations in their macroscopic differential form:

$$\begin{aligned} \nabla \cdot \mathbf{D}(\mathbf{r},t) &= \rho_{\text{ext}}, \\ \nabla \cdot \mathbf{B}(\mathbf{r},t) &= 0, \\ \nabla \times \mathbf{E}(\mathbf{r},t) &= -\frac{\partial \mathbf{B}(\mathbf{r},t)}{\partial t}, \\ \nabla \times \mathbf{H}(\mathbf{r},t) &= \mathbf{j}_{\text{ext}}(\mathbf{r},t) + \frac{\partial \mathbf{D}(\mathbf{r},t)}{\partial t}, \end{aligned} \tag{2.1}$$

where $\mathbf{D}(\mathbf{r},t)$ - electric displacement field, $\mathbf{B}(\mathbf{r},t)$ - magnetic induction, $\mathbf{E}(\mathbf{r},t)$ - electric field, and $\mathbf{H}(\mathbf{r},t)$ - magnetic field, ρ_{ext} - external charge and $\mathbf{j}_{\text{ext}}$ current densities. In vacuum, $\mathbf{D}(\mathbf{r},t)$ and $\mathbf{H}(\mathbf{r},t)$ are linearly proportional to $\mathbf{E}(\mathbf{r},t)$ and $\mathbf{B}(\mathbf{r},t)$ with the vacuum electric permittivity ε_0 and magnetic permeability μ_0 as coefficients, respectively. These constants are approximately $8.854 \cdot 10^{-12}$ F/m and $1.257 \cdot 10^{-6}$ H/m. In matter, however, intrinsic properties such as polarization $\mathbf{P}(\mathbf{r},t)$ and magnetization $\mathbf{M}(\mathbf{r},t)$ fields must be included:

$$\begin{aligned} \mathbf{D}(\mathbf{r},t) &= \varepsilon_0 \mathbf{E}(\mathbf{r},t) + \mathbf{P}(\mathbf{r},t), \\ \mathbf{H}(\mathbf{r},t) &= \frac{1}{\mu_0}\mathbf{B}(\mathbf{r},t) - \mathbf{M}(\mathbf{r},t). \end{aligned} \tag{2.2}$$

Polarization and magnetization fields emerge from the redistribution of charges inside material (referred as internal charges), while charge and current densities in equations 2.1 are generated by the external charges. In optics, external charges are set to zero and non-magnetic materials are typically used.

In a homogeneous, isotropic, and non-magnetic medium, applying the curl operator to the last two equations in 2.1 and combining them yields the wave equation:

$$\nabla \times \nabla \times \mathbf{E} = -\mu_0 \frac{\partial^2 \mathbf{D}}{\partial t^2}. \tag{2.3}$$

A similar equation can be derived for $\mathbf{B}$. The simplest solution of this wave equation is:

$$\mathbf{E}(\mathbf{r},t) = \mathbf{E}_0 e^{i(\mathbf{kr}-\omega t)}, \tag{2.4}$$

which represents a plane wave propagating along the wave vector $|\mathbf{k}| = 2\pi/\lambda$, where λ is the vacuum wavelength. Other solutions to equation 2.3 are more cumbersome, yet it is always possible to decompose them into a linear combination of plane waves, which is called a principle of superposition.

Since all materials in real life are dispersive, the non-locality in space and time must be taken into account. Often, a Fourier transform is applied to the respective fields (e.g. $\mathbf{E}(\mathbf{r},t) = \int \mathbf{E}(\mathbf{r},\omega)e^{-i\omega t}d\omega$) to enter the frequency domain and simplify the representation of the electromagnetic equations. In the absence of external charges and currents,

Maxwell's equations in the Fourier domain read as:

$$\begin{aligned} \nabla \cdot \mathbf{D}(\mathbf{r},\omega) &= 0, \\ \nabla \cdot \mathbf{B}(\mathbf{r},\omega) &= 0, \\ \nabla \times \mathbf{E}(\mathbf{r},\omega) &= i\omega \mathbf{B}(\mathbf{r},\omega), \\ \nabla \times \mathbf{H}(\mathbf{r},\omega) &= -i\omega \mathbf{D}(\mathbf{r},\omega). \end{aligned} \tag{2.5}$$

The following material equations are linking the fields together in isotropic and linear medium:

$$\begin{aligned} \mathbf{j} &= \sigma(\mathbf{r},\omega)\mathbf{E}, \\ \mathbf{B} &= \mu_0 \mu(\mathbf{r},\omega)\mathbf{H}, \\ \mathbf{P} &= \varepsilon_0 \chi(\mathbf{r},\omega)\mathbf{E}, \end{aligned} \tag{2.6}$$

where $\sigma(\mathbf{r},\omega)$ - electric conductivity, $\mu(\mathbf{r},\omega)$ - magnetic relative permeability, and $\chi(\mathbf{r},\omega)$ - dielectric susceptibility. In the current work non-magnetic materials are used, which sets $\mu = 1$. By combining the last equation from the set 2.6 with the first equation in 2.2, one can obtain the fundamental material equation:

$$\mathbf{D}(\mathbf{r},\omega) = \varepsilon_0 \varepsilon(\mathbf{r},\omega)\mathbf{E}(\mathbf{r},\omega) \tag{2.7}$$

Here relative permittivity was denoted via susceptibility with a simple equation $\varepsilon = 1 + \chi$. Generally, dielectric permittivity is a complex function. Its imaginary part determines the phase changes as well as the optical absorption of the electromagnetic wave propagating through a medium.

In a homogeneous and non-magnetic medium, by using identity $\nabla \times (\nabla \times \mathbf{F}) = \nabla(\nabla \cdot \mathbf{F}) - \Delta\mathbf{F}$ and combining it with the material equation 2.7, wave equation 2.3 takes the following form in the Fourier domain:

$$\mathbf{k}(\mathbf{k} \cdot \mathbf{E}) - k^2 \mathbf{E} = -\varepsilon(\omega)\frac{\omega^2}{c^2}\mathbf{E}, \tag{2.8}$$

where $c = (\varepsilon_0 \mu_0)^{-\frac{1}{2}}$ is the speed of light in vacuum. We are most interested in solutions where the electric field is perpendicular to the direction of propagation, called transverse. For transverse waves $(\mathbf{k} \cdot \mathbf{E}) = 0$ due to $\Delta \cdot \mathbf{E} = 0$ (and, $\mathbf{k} \perp \mathbf{E} \perp \mathbf{B}$ due to $\Delta \cdot \mathbf{B} = 0$). This yields the basic dispersion relation for the free space wave:

$$k_0^2 = \varepsilon\left(\frac{\omega}{c}\right)^2. \tag{2.9}$$

The refractive index is as $n = \sqrt{\varepsilon}$ and is generally a complex function.

Polarization of light

For a transverse electromagnetic plane wave, the electric field $\mathbf{E}$ is perpendicular to the direction of propagation $\mathbf{k}$. One of the most significant properties of transverse waves is polarization, which refers to the orientation of the oscillations of the electric field vector.

Consider a plane wave propagating in the positive z direction. The electric field vector $\mathbf{E}$ can be written as the superposition of the two linearly independent vectors $\mathbf{E}_x$ and $\mathbf{E}_y$. In the general case, $\mathbf{E}_x$ and $\mathbf{E}_y$ are complex with real parts containing the information about the amplitudes and imaginary parts about the phases. The state of polarization of an electromagnetic wave can be classified based on the relationship between the amplitudes and phases of these components. Specifically, the wave can be linearly, circularly, or elliptically polarized:

- **Elliptical polarization**: In the general case where the amplitudes are not equal or the phase difference is not exactly $\pi/2$, the tip of the electric field vector traces out an ellipse in the plane perpendicular to the direction of propagation. The shape and orientation of the ellipse are determined by the relative amplitudes and phase difference of $\mathbf{E}_x$ and $\mathbf{E}_y$.

- **Linear polarization**: This occurs when the components $\mathbf{E}_x$ and $\mathbf{E}_y$ are in phase or exactly out of phase. In this case, the electric field vector oscillates along a single line, which can be at any angle to the x axis depending on the relative amplitudes of $\mathbf{E}_x$ and $\mathbf{E}_y$.

- **Circular polarization**: This is a special case of elliptical polarization that occurs when the amplitudes of $\mathbf{E}_x$ and $\mathbf{E}_y$ are equal, and the phase difference between them is exactly $\pi/2$. The electric field vector rotates in a circle in the plane perpendicular to the direction of propagation.

In this thesis, the receiver perspective is used to describe polarization states, which allows us to define right and left circularly polarized light. If the electric field vector rotates clockwise, the light is right circularly polarized (RCP). Conversely, if the electric field vector rotates counterclockwise, the light is left circularly polarized (LCP). The different states of light polarization are shown schematically in Figure 2.1. It is worth mentioning that natural light, such as sunlight, is typically unpolarized, meaning that its electric field oscillates in random directions.

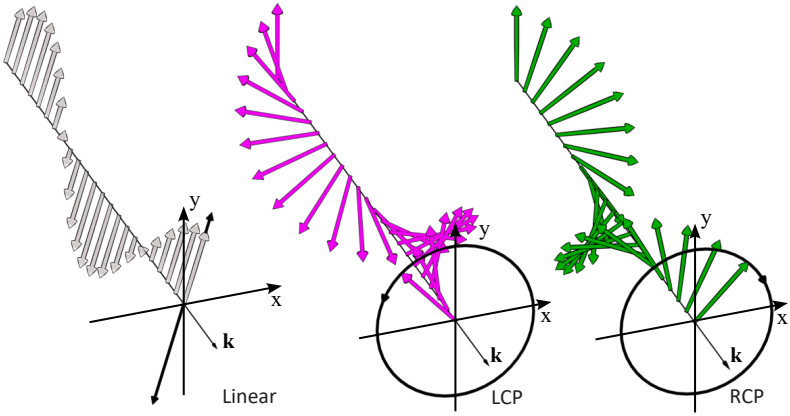

Figure 2.1: Artistic illustration of different polarization states of light. White arrows represent propagation of linearly polarized light, magenta and olive arrows depict the evolution of an electric field **E** during the propagation of left (LCP) and right circularly polarized (RCP) light.

2.1.2 Optics of metals

The following discussion emphasizes the classical origins of the optical properties of metals and introduces surface plasmon polaritons.

Drude model of free electron gas

The Drude model is a remarkably simple yet powerful tool for describing the electromagnetic response of metals over a broad spectral range. In this model, the "free" electron gas determines the interaction of light with the metal.

To determine the dielectric function of metals, consider $\mathbf{r}$ as the displacement of a single electron. The electron begins to oscillate in response to the driving external electric field, allowing a simple equation of motion to be written:

$$m_e\ddot{\mathbf{r}} + m_e\gamma\dot{\mathbf{r}} = e\mathbf{E}_0 e^{-i\omega t}, \tag{2.10}$$

where m_e is the effective electron mass, γ is the damping term due to the electron scattering, and the electric field is assumed to be harmonic. A solution can be found by employing an ansatz $\mathbf{r} = \mathbf{r}_0 e^{-i\omega t}$. Substituting the solution in the macroscopic polarization field $\mathbf{P} = ne\mathbf{r}$, where n is the number of free electrons oscillating per unit volume, and

using the first equation in 2.2, we obtain:

$$\varepsilon(\omega) = 1 - \frac{\omega_p^2}{\omega^2 + \gamma^2} + i\frac{\gamma\omega_p^2}{\omega(\omega^2 + \gamma^2)}. \tag{2.11}$$

Here, the result is expressed with separate real and imaginary parts. The plasma frequency $\omega_p = \sqrt{ne^2/m_e\varepsilon_0}$ plays a critical role in understanding the optical behavior of metals. For frequencies ω lower than ω_p the real part of $\varepsilon(\omega)$ is negative and the external electric field can penetrate the metal only to a very short distance. This explains the high reflectivity of metals in the visible and infrared (IR) regions. Conversely, for $\omega > \omega_p$, electromagnetic waves begin to penetrate the metal, so it becomes transparent, a phenomenon typically observed in the ultraviolet part of the spectrum.

The Drude model can be further refined by considering the atomistic nature of the medium. When the energy of incident photons reaches or exceeds the band gap in metals, electrons in lower energy bands may be excited. Interband transitions and all other types of material resonances, such as phonons, can be accounted for by adding additional terms to the left-hand side of the equation 2.10, known as Lorentz oscillators. Thus, the dielectric function can be extended with multiple oscillators to fit experimental data for specific materials [40]. In addition, replacing the term 1 in the real part of $\varepsilon(\omega)$ with ε_∞ accounts for substantial polarization fields between ion cores and higher electronic orbitals, especially in noble metals [15].

A crucial aspect of the complex permittivity for any material is that its real and imaginary parts are not independent from each other, and are linked through the Kramers–Kronig relations [40].

Surface plasmon polaritons

The wave equation 2.3 can be transformed into the Helmholtz equation using the identity $\nabla \times \nabla \times \mathbf{E} = \nabla(\nabla \cdot \mathbf{E}) - \nabla^2\mathbf{E}$ and assuming a time harmonic electric field:

$$(\nabla^2 + \varepsilon k_0^2)\mathbf{E} = 0. \tag{2.12}$$

Consider a planar interface between a metal and a dielectric medium, with the origin placed at the boundary. The x-axis runs along the interface, and the z-axis is normal to it. Let the indices $j = 1, 2$ denote the metal and dielectric properties, respectively. The dielectric function of the metal is the a complex function $\varepsilon_1 = \varepsilon_1' + \varepsilon_1''$, where ε_1' and ε_1'' are real and $|\varepsilon_1''| \ll |\varepsilon_1'|$. The permittivity of the dielectric ε_2 is assumed to be real. We look for solutions of the Helmholtz equation 2.12 that are localized and propagate along the interface. By solving the Helmholtz equation with appropriate boundary conditions,